Supplement of Biogeosciences Discuss., 12, 11113–11157, 2015
http://www.biogeosciences-discuss.net/12/11113/2015/
doi:10.5194/bgd-12-11113-2015-supplement

Biogeosciences
Discussions
Open Access

Supplement of

The role of snow cover and soil freeze/thaw cycles affecting boreal-arctic soil carbon dynamics

Y. Yi et al.

Correspondence to: Y. Yi (yonghong.yi@ntsg.umt.edu)

Table S2 The model prescribed fraction (percentage) of leaf, fine root and woody components of litterfall for each model biome type based on White et al. (2000).

Biome type	Leaf (%)	Fine roots (%)	Wood (%)
Tundra	32	48	20
Forest-tundra	28	42	30
Taiga-boreal	24	36	40
Grasslands/steppe/Shrubland	28	42	30
Wetland	36	54	10
Deciduous/mixed forest	24	36	40

Table S3 Prescribed labile, cellulose and lignin fractions (percentage) of leaf, fine root and woody litterfall (White et al. 2000), used to partition model litterfall and relative decomposability in the soil decomposition model.

	Labile (%)	Cellulose (%)	Lignin (%)
Leaf	55	31	14
Fine roots	34	44	22
Wood	0	71	29

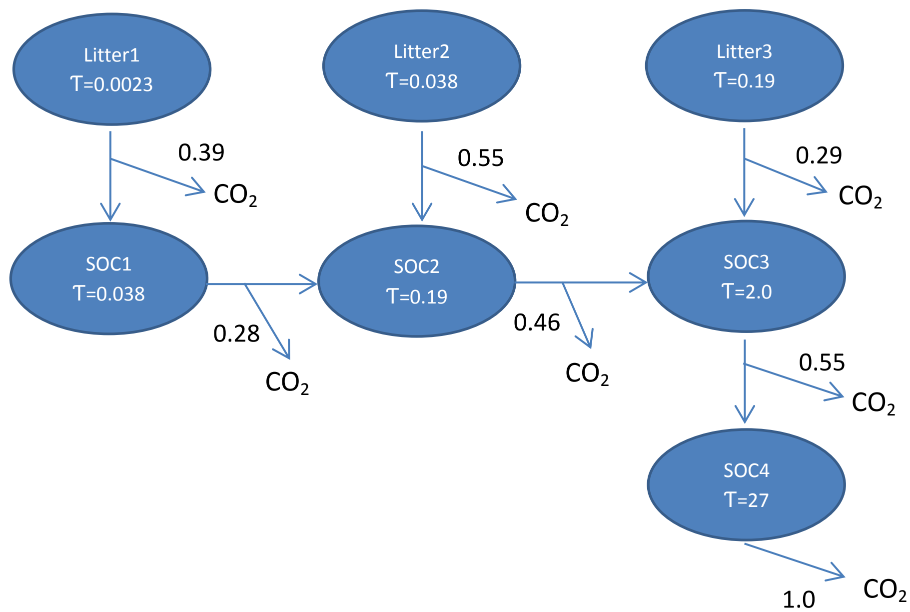

Figure S1. The pool structure, transitions, respired fractions (numbers on the arrows) and turnover rates for the soil organic carbon (SOC) decomposition model (numbers in the ellipses, yr^{-1}). The SOC pools include 3 litterfall pools, 3 SOC pools with relatively fast turnover rates (SOC1-3) and a deep SOC pool (SOC4) with relatively slow turnover.

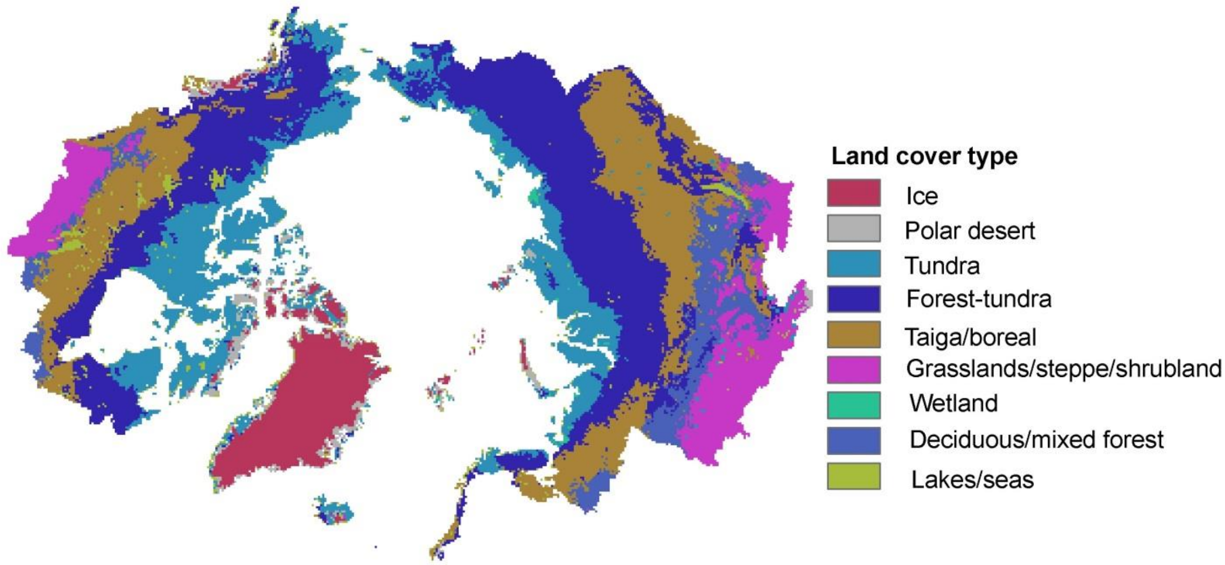

Figure S2. The merged land cover map based on the MODIS Collection 5 IGBP (International Geosphere-Biosphere Programme) land cover and the Circumpolar Arctic Vegetation Map (CAVM) classifications. Tundra, forest-tundra and taiga/boreal biomes account for 18.1%, 31.4% and 20.0% of the pan-Arctic basin and Alaska study area, respectively.

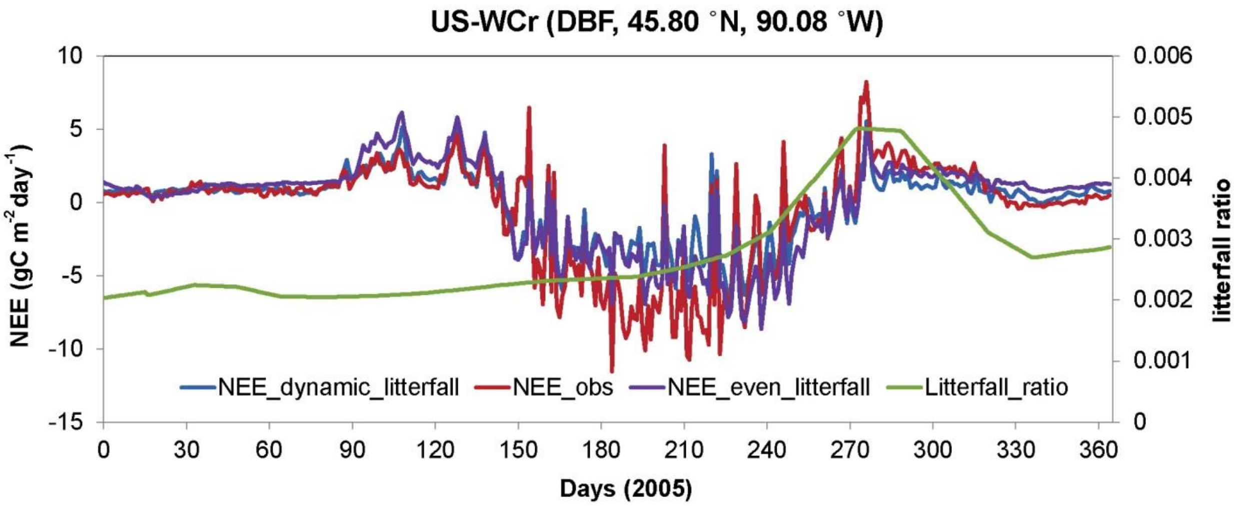

Figure S3. Comparisons of simulated NEE fluxes using dynamical litterfall allocation and evenly distributed litterfall schemes at a deciduous broadleaf forest (DBF) tower site. The dynamic litterfall allocation scheme was based on satellite NDVI (normalized difference vegetation index) time series (Appendix A2), and the daily proportion of annual total litterfall is shown as Litterfall_ratio. NEE_obs indicates the tower observed NEE fluxes, NEE_dynamic_litterfall and NEE_even_litterfall represent model simulated NEE fluxes using the dynamic litterfall allocation and evenly distributed litterfall schemes, respectively.

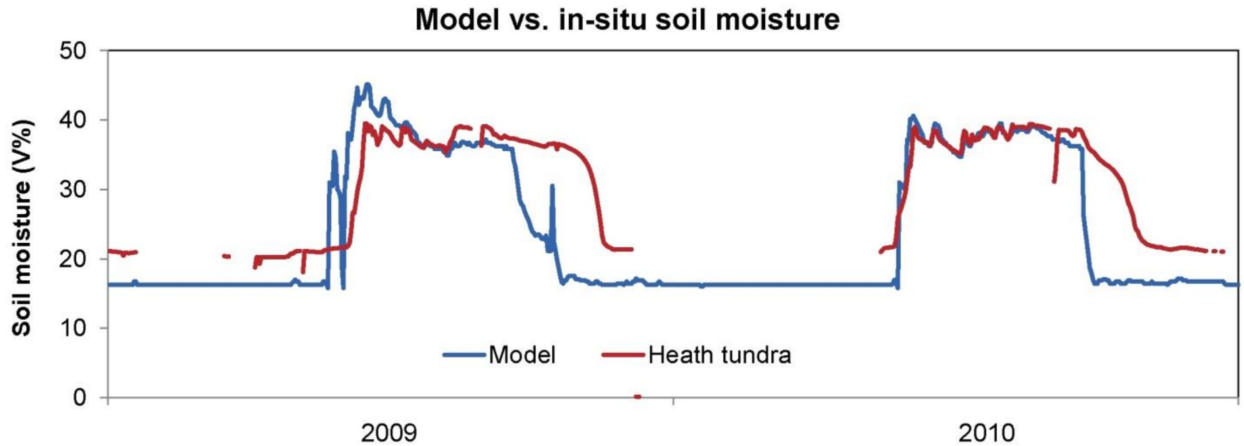

Figure S4. Comparisons of model simulated surface soil moisture (~ 5 cm depth) and in situ measurements at the Imnavait Creek, Alaska, tundra tower validation site. Only the measurements at the dry heath tundra site were included due to paucity of soil moisture data at the other two tundra sites. The year 2008 was not included due to relatively few measurements available at the dry heath tundra site. Generally, different soil moisture datasets are not directly comparable due to different statistical moments and systematic bias. Therefore, the modeled and in situ soil moisture records were scaled to a consistent mean and standard deviation before comparisons following Koster et al. (2009). Note that the simulated soil moisture during the winter was much lower than the tower measurements prior to the scaling.

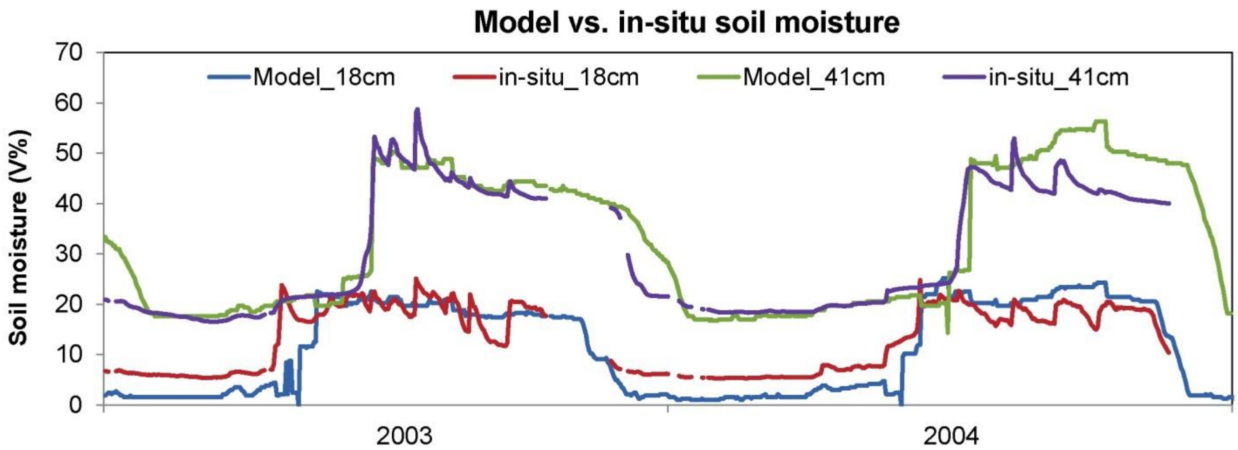

Figure S5. Comparisons of model simulated soil moisture at different depths (18, 41cm) and in situ measurements at a mature boreal forest site in Manitoba, Canada. The year 2002 was not included due to relatively few measurements available for that year. Similar as Fig. S4, the simulated soil moisture was rescaled to match the mean and standard deviation of the in situ soil moisture data prior to the comparison.

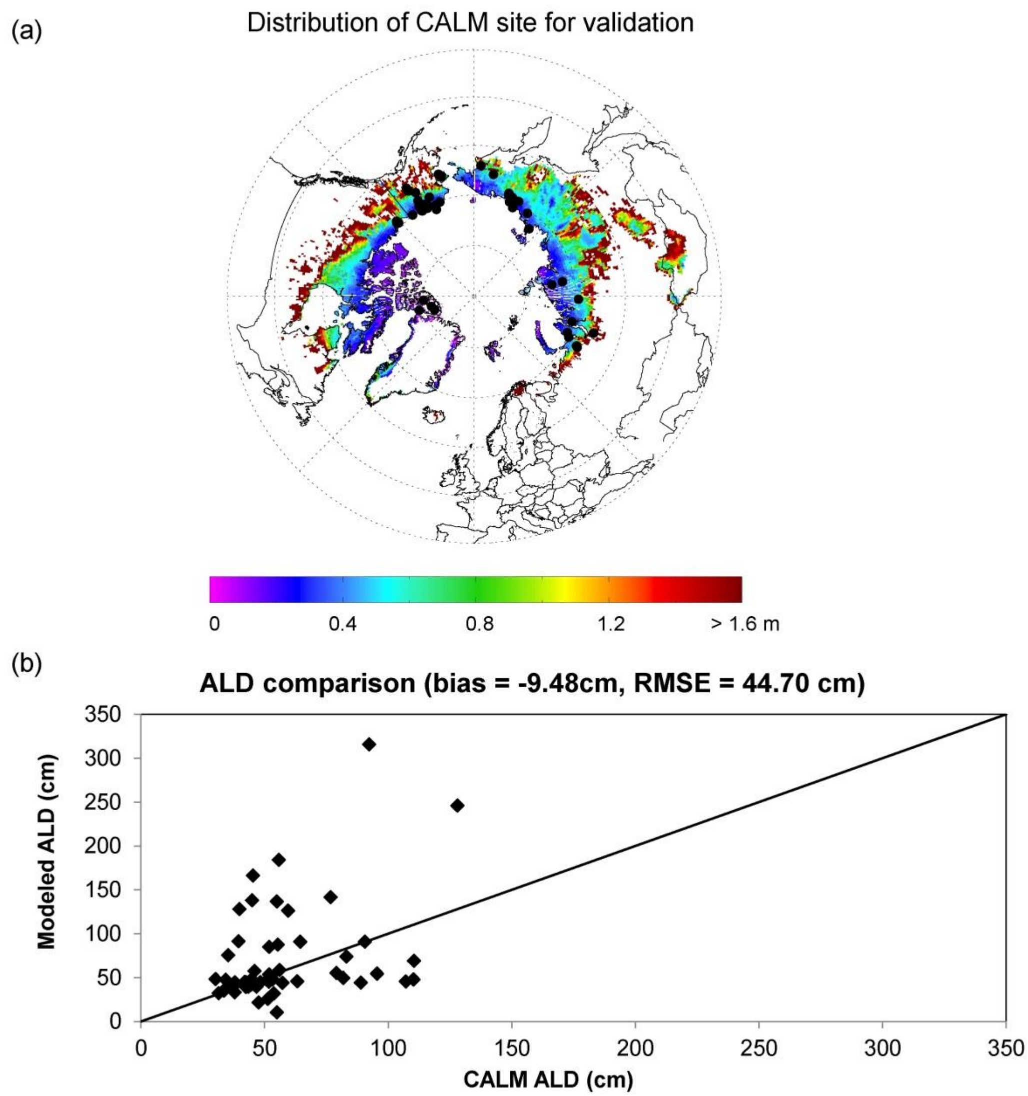

Figure S6. (a) Distribution of 53 Circumpolar Active Layer Monitoring (CALM) tundra sites (as indicated by black dots) used for model active layer depth (ALD) validation; (b) Comparisons of model simulated ALD versus the CALM observations. The distribution of CALM sites was shown over the model simulated mean (1982-2010) ALD map. The comparisons were made at different periods from 1982 to 2010 since CALM observations span different periods.

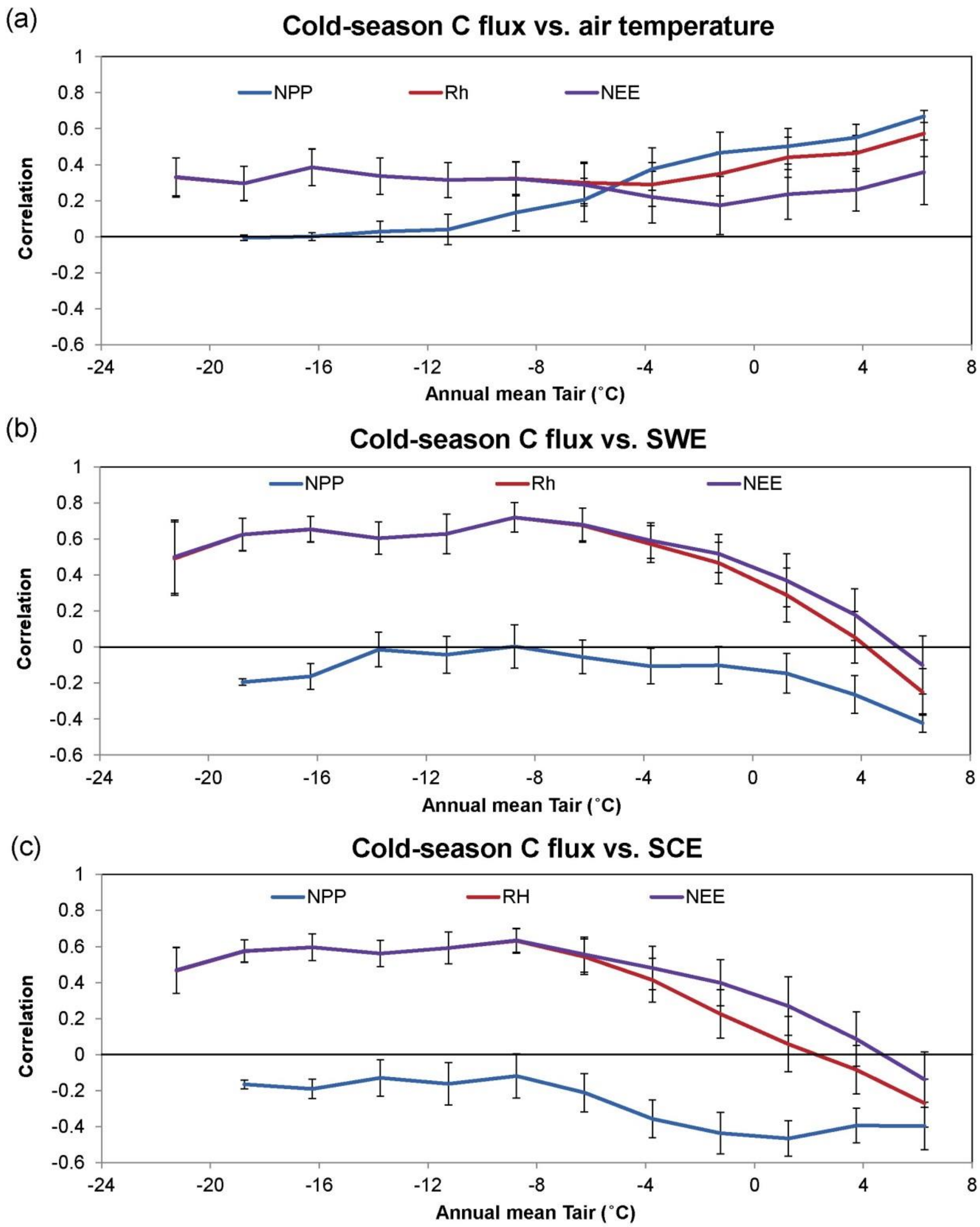

Figure S7. Correlations between cold-season (from November to April) carbon fluxes and climate variables including cold-season air temperature (Tair), snow water equivalent (SWE) and snow cover extent (SCE). The correlations were binned into 2.5 °C intervals of annual mean Tair. The standard deviation of correlations across each climate zone is shown through the error bars.

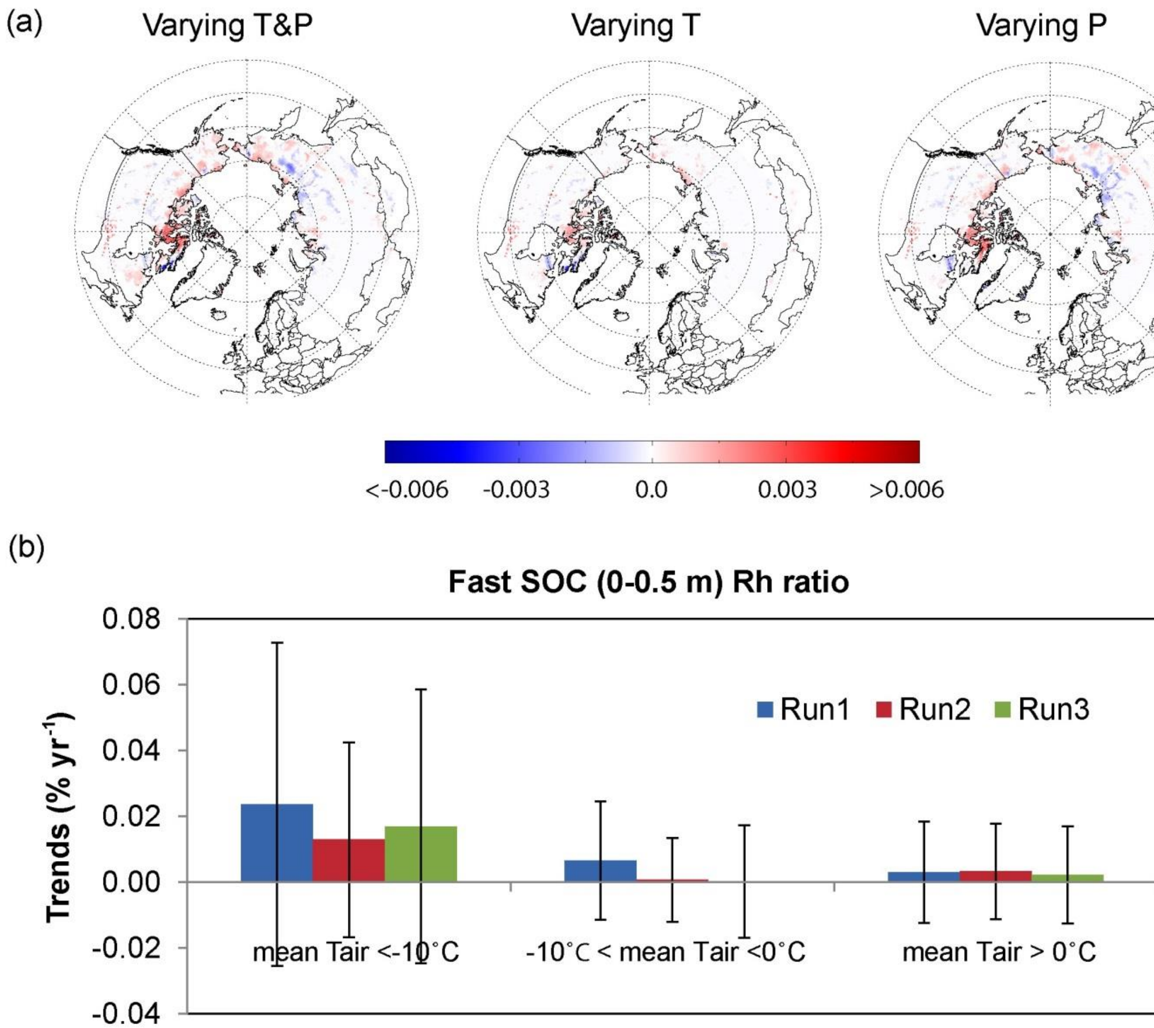

Figure S8. (a) Simulated temporal trends (unit: yr^{-1}) in the ratio of the warm-season (May-October) Rh (soil heterotrophic respiration) contribution from the upper soil (≤0.5m) organic carbon (SOC) pool to total Rh for the model sensitivity analysis runs from 1982 to 2010. The zonal-averages of Rh ratio trends for the sensitivity analysis are shown in (b). For the sensitivity analysis, the model was driven using different surface meteorology datasets. Run1 indicates model simulations based on varying air temperature (T) and precipitation (P) inputs; Run2 indicates model simulations based on varying T inputs alone; and Run3 indicates the model simulations based on varying P inputs alone.

References

Koster, R. D., Guo, Z. C., Yang, R. Q., Dirmeyer, P. A., Mitchell, K., and Puma, M. J.: On the Nature of Soil Moisture in Land Surface Models, J Climate, 22, 4322-4335, 2009.